

## ADVANCES IN SOLAR CHIMNEY TURBINE MODELLING

Leonardo P. Rangel<sup>a</sup>, Bruno A. Contessi<sup>b</sup>, Tomás A. Copes<sup>c</sup>, Patricio Alberto<sup>d</sup> and  
Karolline Ropelato<sup>e</sup>

<sup>a</sup>ESSS, Engineering Simulation Scientific Software, Av. Presidente Vargas, 3131, Rio de Janeiro, Brazil,  
[leonardo@esss.com.br](mailto:leonardo@esss.com.br), <http://www.esss.com.br/>

<sup>b</sup>ESSS, Engineering Simulation Scientific Software, Av. Presidente Vargas, 3131, Rio de Janeiro, Brazil,  
[bruno.contessi@esss.com.br](mailto:bruno.contessi@esss.com.br), <http://www.esss.com.br/>

<sup>c</sup>ESSS, Engineering Simulation Scientific Software, Baltimore 645, Villa Allende, Córdoba, Argentina,  
[tomas@esss.com.br](mailto:tomas@esss.com.br), <http://www.esss.com.br/>

<sup>d</sup>ESSS, Engineering Simulation Scientific Software, Baltimore 645, Villa Allende, Córdoba, Argentina,  
<http://www.esss.com.br/>

<sup>e</sup>ESSS, Engineering Simulation Scientific Software, Av. Presidente Vargas, 3131, Rio de Janeiro, Brazil,  
[ropelato@esss.com.br](mailto:ropelato@esss.com.br), <http://www.esss.com.br/>

**Keywords:** Solar chimney, CFD, Gannon Method, Fluri Method

**Abstract.** Solar chimneys are one of the cleanest forms of power generation that are technologically feasible today. Many studies have been published since the operation of the prototype of Manzanares in the 1980s showing that the major geometric system parts contributes differently for obtaining the maximum overall efficiency in terms of power generation. It can be seen that the higher the tower or chimney and also the solar collector area the greater the amount of energy to be generated. It is also known that any solar chimney to be built should have a turbine coupled, however the performance of such turbines has not been thoroughly studied. Geometric details and constructive parameters of the turbines are essential for the greatest possible conversion of turbulent kinetic energy from the heated air into potential energy. This work evaluates different arrangements of turbines considering both their positioning and their geometric details through computational fluid dynamics and concludes that it is possible to offer the energy market an arrangement that is innovative and efficient.

## 1. INTRODUCTION

Among the more traditional forms of renewable energy are wind and solar. A combination of these allows you to take advantage of the heated air to produce energy sustainably.

A power system with the use of a solar chimney is known as Solar Updraft Power Plant (SUPP). It enables the conversion of sunlight into electricity by three physical principles related to air, greenhouse, buoyancy and turbulence. Since the flow of fresh air from the atmosphere may be partially confined and heated by solar radiation and which, when heated, air increases its speed and transfers thermal energy to kinetic energy and potential energy to then , one can obtain clean energy renewable and, it seems, without any negative effect to the environment.

Since about 1500 the principles described above were observed by Leonardo da Vinci and many other scientists have cited or developed inventive ideas to enhance this system to generate over the years, as the work of reviewing (Dhahri & Omri, 2013).

The most relevant work area to current scientific means occurred in 1982 when a group of engineers led by Jörg Schlaich developed and operated the largest reference solar chimney cited in scientific and technical publications was the prototype of Manzanares (Ciudad Real, Spain) (Schlaich, 1995).

From Manzanares, different approaches have emerged highlighting the major parts of the solar chimney systems, chimney or tower, pickup and turbine. Aiming to analyze progress on the models of turbines employed it was found that for this design, a vertical-axis turbine with simple step (single vertical axis turbine) blades and only four drivers without flow (loose translation for IGV, inlet was used guide vanes).

Some jobs have replaced the mathematical modeling of flow through the turbine in their simulations for values of the coefficient of pressure loss, as due to the reduction in area at the position of the vertical axis turbines, this device allowed a large computational savings and a significant reduction in the complexity of mathematical model.

Gannon has developed a theoretical and experimental study about the performance of a solar chimney power plant focused on the operational range of a full-size plant and on the limitations of a vertical axis single turbine. Detailed design of turbine with rotor tip stagger angle and inlet guide vanes (IGVs) flat angle had provide the starting torque for the studied case with flow and load coefficients. It has been analyzed the positive use of IGVs as structure to reduce kinetic energy losses. Its work has presented successfully calculated total-to-total and total-to-static efficiencies for operational conditions of low and high pressures on the turbine (Gannon, 2002).

Gannon and Von Backström have designed an experimental investigation introducing the pre-swirl by IGVs and reduce the turbine exit turbine kinetic energy at the diffuser inlet (located on the base of the chimney). Detailed work with regards do development of turbine profiles throughout a vertical axis single turbine aided on mapping low and high pressure drops. Results have revealed that favorable diffuser conditions have produced efficiencies up to 90% (Gannon & Von Backström, 2003).

Von Backström and Gannon have analytically investigated the turbine blade row by turbine diffuser loss and load coefficients and degree of reaction to express each coefficient on turbine efficiency. A 720 mm diameter vertical single axis turbine has been evaluated by measurements and analytical results have been validated. Important inputs have been pointed to guarantee initial layouts, sizing and design of solar chimney turbines (Von Backström & Gannon, 2004).

Pretorius (Pretorius, 2004) and Pretorius and Kröger (Pretorius & Kröger, 2006) have mentioned that loss coefficient effect through the turbine inlet is negligible. In their work, authors

have simulated with coefficient between 0.14 and 0.25.

Denantes and Bilgen ([Denantes & Bilgen, 2006](#)) have compared off-design performance model for counter-rotating to single-runner turbines. Results have demonstrated that from the efficiency point of view two counter-rotating turbine system will operate with reduced torque on axis and perform under their best efficiency at a solar intensity of less than  $800 \text{ W/m}^2$ . However, single-runner turbine has presented higher nominal efficiency advantage for bigger solar chimney plants.

Ming et al. ([Ming, Liu, Xu, Xiong, Guan, & Pan, 2008](#)) have carried out a study to give a reference for the design of large-scale solar chimney power plant systems. Authors have analyzed a 5-blade turbine with CFD by its power output and turbine efficiency on a 10 MW theoretical power plant (400 m in height and 30 m in radius). Results have shown that 50% of efficiency can be reached, although authors have stated that such 5-blade turbine may be unsuitable to put into practice due to its unstable operation conditions under rotational speed higher than 40 rpm (peak efficiency).

Fluri ([Fluri, 2008a](#)) and Fluri and Von Backström ([Fluri & Von Backström, 2008b](#)) have analyzed several approaches and layouts for solar chimney turbines such as single and counter-rotating turbines with and without IGVs. Their work has been based on a modelling with various radial sections along the blades which allowed conclusion on the most efficiency turbine system under different speeds. In practical means, they have revealed that counter-rotating turbines can provide highest peak efficiencies only under low speeds and small differences on turbine efficiencies have been observed when compared to single ones, where the presence of IGVs have been highly recommended.

Fluri and Von Backström ([Fluri & Von Backström, 2008c](#)) also studied three different configurations of one or several turbogenerators for a power conversion unit (PCU): single vertical axis, multiple vertical axis and multiple horizontal axis turbine. Among these configurations, single vertical axis turbine presents highest efficiency and energy yield due the reduced loss mechanisms. It was also found out that efficiency differences can be explained by the diffuser area.

Aiming to develop a new turbine system to improve power generation in SUPP scientists and engineers must search in physical parameters and phenomena new design and methodologies to extract the most energy available. In this work, both Gannon's and Fluri's turbine design efficiencies have been compared to the Manzanares prototype by CFD in the same scale.

## 2. METHODOLOGY

Aiming to compare V-A and H-A turbines based in the work of Gannon ([Gannon, 2002](#)) and Fluri ([Fluri, 2008a](#)) both at Manzanares' full size by CFD, this work has firstly reviewed both V-A and H-A turbine designs and has suggested a proper design fit to the Manzanares' scale. The redesign started with a complete review on the construction system of both turbines, this work has been divided into:

- a) Development of Gannon's turbine;
- b) Development of Fluri's turbine.

### 3. DEVELOPMENT OF GANNON'S TURBINE

The turbine is one of the main sub-systems of a solar chimney power plant. Other systems are the solar collector, the chimney and the generator (see Figure 1). Air heated in the solar collector surrounding the chimney enters it radially through passages between the pillars supporting the chimney. The pillars may be airfoil shaped and arranged along non-radial chord lines, to act inlet guide vanes (see Figure 1). The typical solar chimney turbine is of the axial flow type. The main function of the turbine is the efficient conversion of fluid power to shaft power. A secondary function of solar chimney turbines is flow and output power control by adjustment of its blade angles.

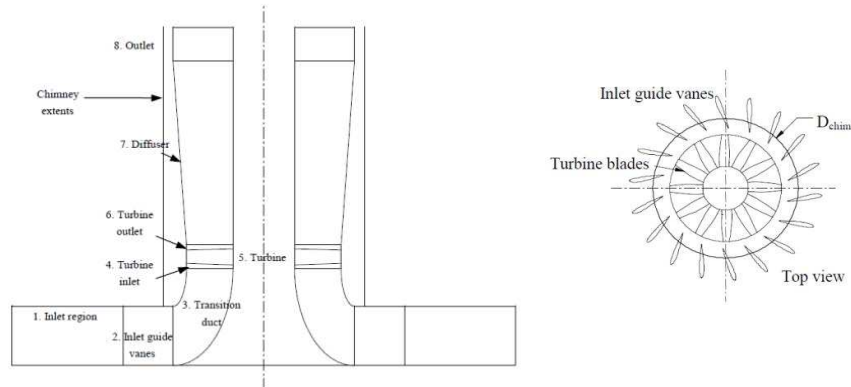


Figure 1: Scheme of Gannon's system.

Gannon has worked on the turbine characteristics focused on dimension following these steps:

- A 1D simple analysis developed to obtain an estimation on the turbine performance;

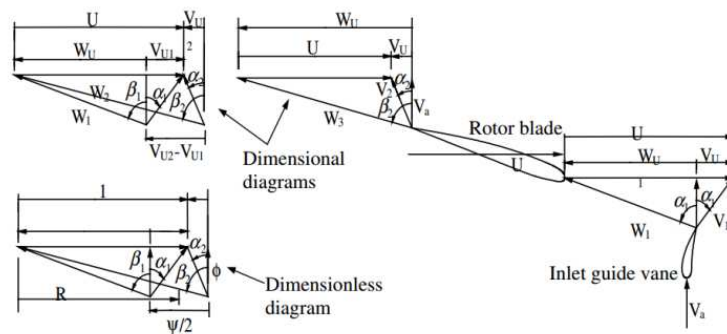


Figure 2: Turbine velocity diagrams.

Consider the velocity diagrams (see Figure 2). The following conventions apply:

- The axial velocity component  $V_z$  is vertically upwards.
- The blade velocity  $U$  is from left to right.
- Velocity components parallel to the blade velocity are positive in the direction of the blade velocity.

- Flow angles are measured from the axial direction to a vector pointing away from the axis.
- Flow angles to the right (left) of the axis are positive (negative).
- Turbine diameter (720 mm), rotation velocity and tip/hub coefficient are optimized for the turbine operation range;
- A 2D simple analysis has been applied to have inlet and outlet turbine blades angles (see [Figure 4](#) and [Figure 5](#));
- A complementary 1D study with regards to coupling the SIMPLEX optimization algorithm has been applied to define the blade profiles based on NACA 4-digit (see [Figure 3](#)).

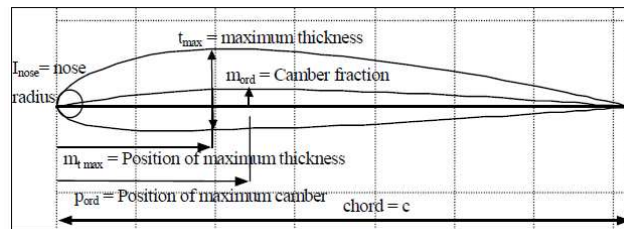


Figure 3: Naca airfoil characteristics.

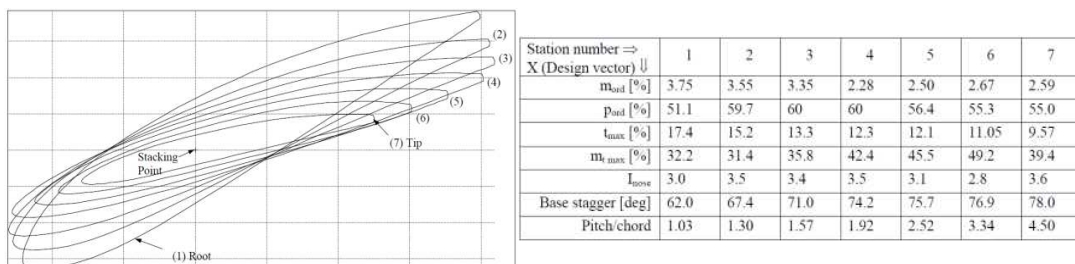


Figure 4: Airfoil distribution in rotor blade of Gannon's system.

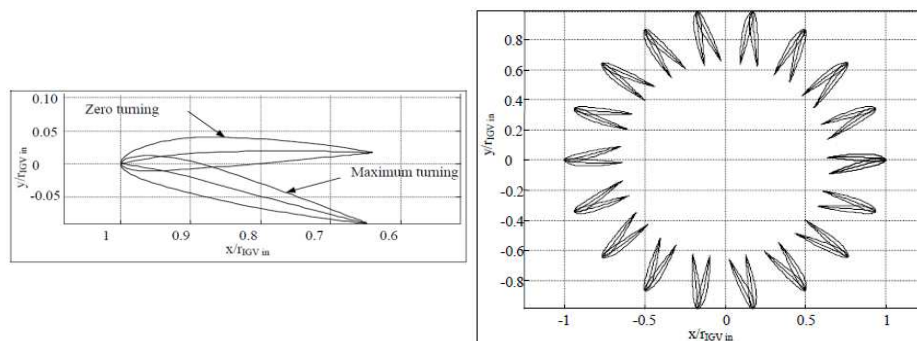


Figure 5: Airfoil angle in the IGV.

#### 4. DESIGN OF GANNON'S TURBINE ON THE MANZANARES SCALE.

Data about the original geometry of the Manzanares' plant was not sufficient for complete rebuilding the axial turbine (vertical axis) used for power generation. Thus, some assumptions and modifications have been performed on the turbine structure. [Figure 6](#) and [Figure 7](#) show geometry details and mesh periodic volume of Gannon's system to Manzanares adapted to scale.

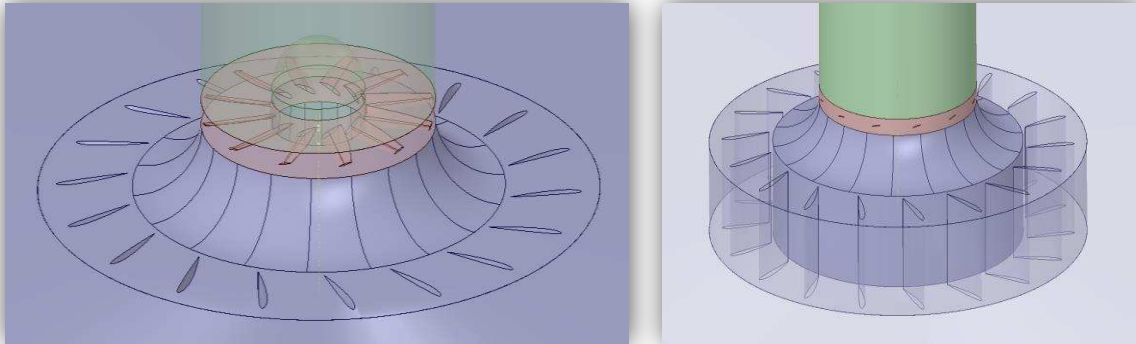


Figure 6: Geometry details of Gannon's system to Manzanares scale.

The full geometry has been rebuilt and simulated with the commercial software ANSYS CFD for several rotation speeds aiming to obtain the operation curve for the system (turbine + IGV + chimney). Simulation configuration has been set as below:

Domains:

- Steady state: collector, chimney, farfields, turbine, IGV (slice of 1/18);
- Rotation: rotor (slice of 1/12).

[Figure 7](#) provides a view of the periodic system (left), detailed rotor mesh (right up) and detailed IGV mesh (right down). The methodology applied to the simulation was to map the load loss through mass flow curves for several different rotations and then use these results to represent the rotor in a 2D simulation of the solar chimney system.

Simulations of the rotor and IGV separately with nozzle speeds of 2, 4, 6, 8, 10, 12 and 14  $\text{m}\cdot\text{s}^{-1}$  provided fixed output pressure drop, velocity and temperature on the diffuser. These simulations allowed obtaining radial velocity and turbulence fields in the rotor inlet at each speed. For each turbine load loss curve (rotation speed) a different solar chimney simulation has been developed. Thus, one obtains a full curve of plant operating conditions for each turbine rotation.

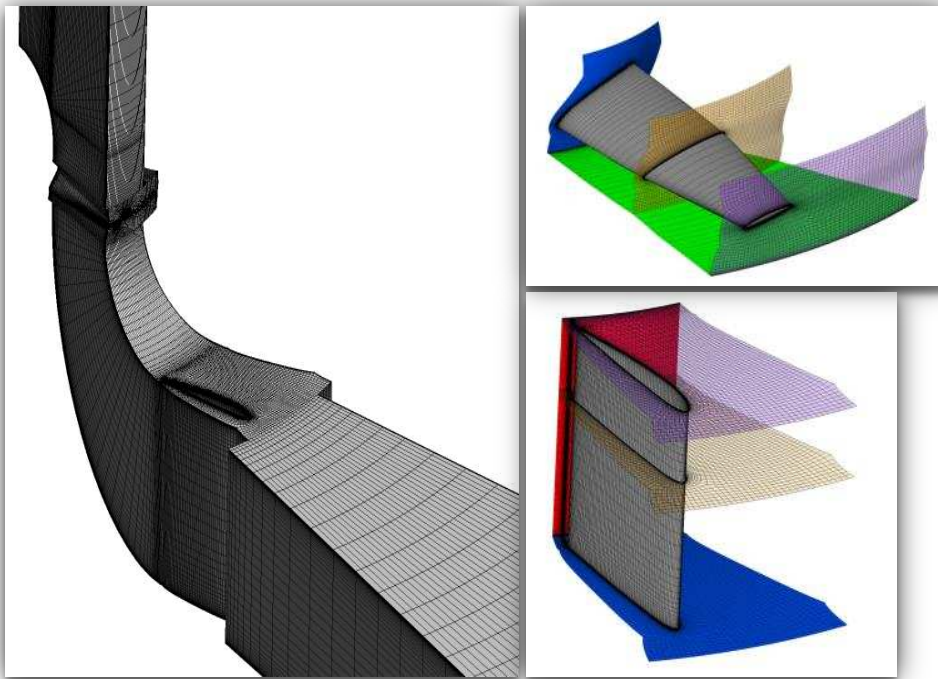


Figure 7: Mesh on periodic volume of Gannon's system to Manzanares scale.

The mesh was built on ANSYS ICEM CFD and ANSYS TurboGrid.

- Full hexa mesh.
- Elements/Nodes: 3,3 millions.

The simulation was developed by Ansys CFX 15.0 (see [Figure 8](#)).

- Models
  - Fluid: Incompressible Air.
  - Density: 1,1613 kg/m<sup>3</sup>
  - Turbulence: SST
  - Heat Transfer: None
  - Interfaces: Stage
- Boundary Conditions
  - Inlet: Opening ( $P_{rel} = 0$  Pa)
  - Outlet:  $V_{flow} = \text{Volume Flow Rate} / 18$
  - Heat Flux: 320 W/m<sup>2</sup>

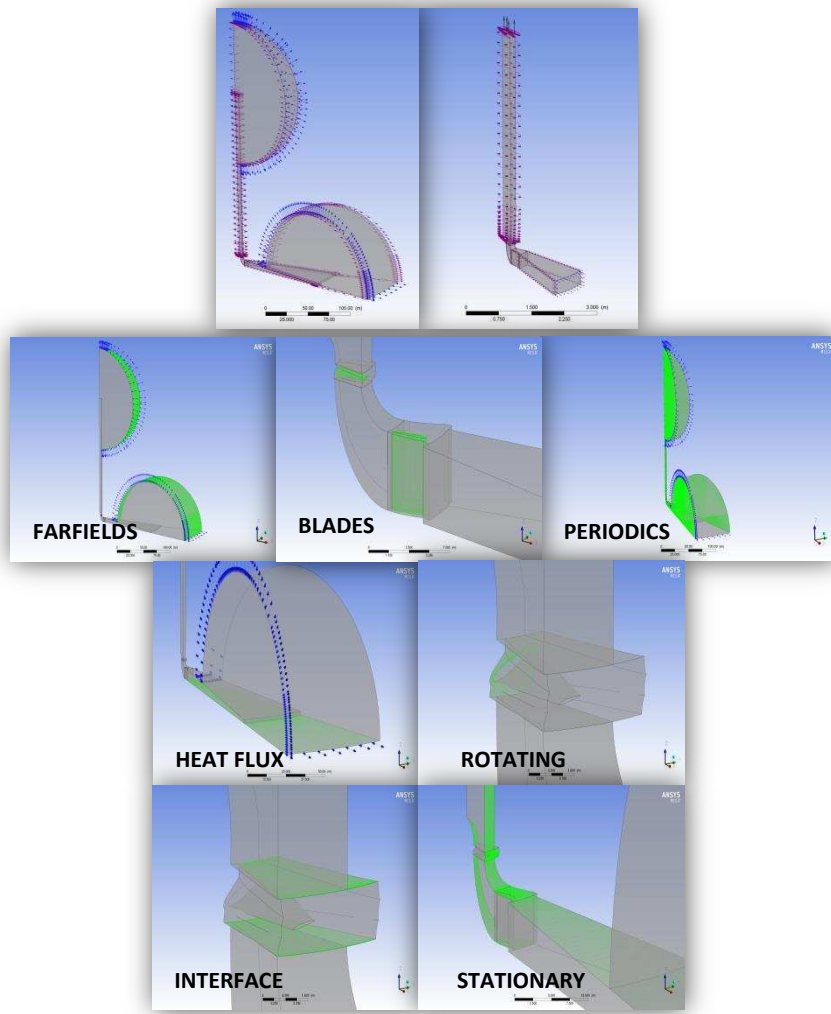


Figure 8: CFD boundaries Setup of Gannon's system.

Figure 9 shows a typical plot of the velocity field simulation in the 2D model. Scale has been removed since detailed results are proprietary. Nevertheless, red color indicates highest velocity near the turbine positioning and dark blue color indicates lowest velocity in the farfield region, outside the system (collector + chimney).

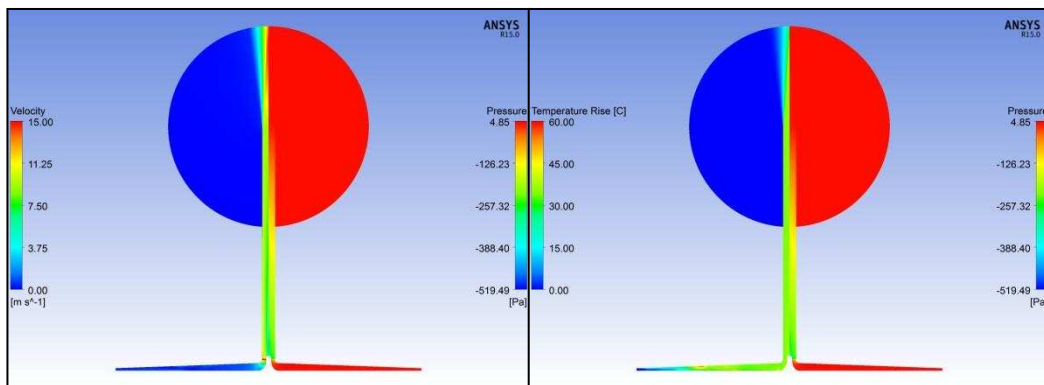


Figure 9: Velocity, temperature and pressure distribution in chimney.

Results presented in **Chart 1** shows a maximum shaft power of 78 kW at 8 rad.s<sup>-1</sup> for Manzanares' system. It presents simulation results of axis torque and the shaft power for the full domain rotor (12 blades) applied for a range of rotations applied to vertical axis turbine for Manzanares' scale. At 8 rad s<sup>-1</sup> (about 58 rpm) the maximum shaft power of 78 kW has been achieved with 9.75 kNm of axis torque. As reference, the maximum axis torque has been achieved at 6 rad s<sup>-1</sup> (about 76 rpm) with 73 kW of shaft power.

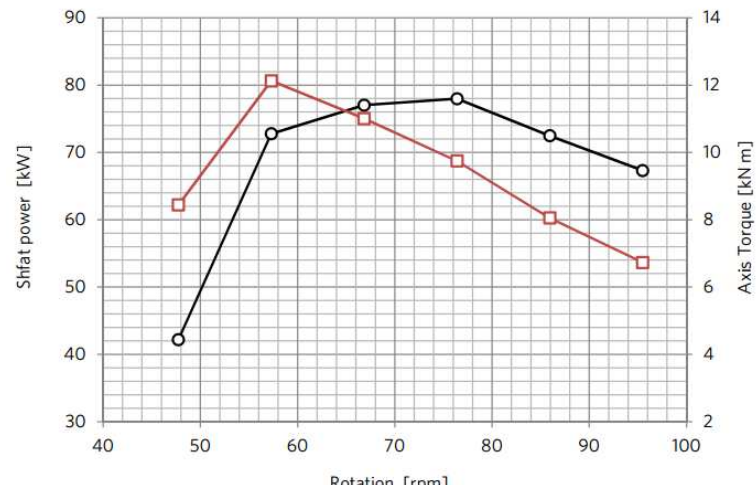


Chart 1: Simulation performances, Torque and Power. Black (Shaft power), Red (Axis Torque).

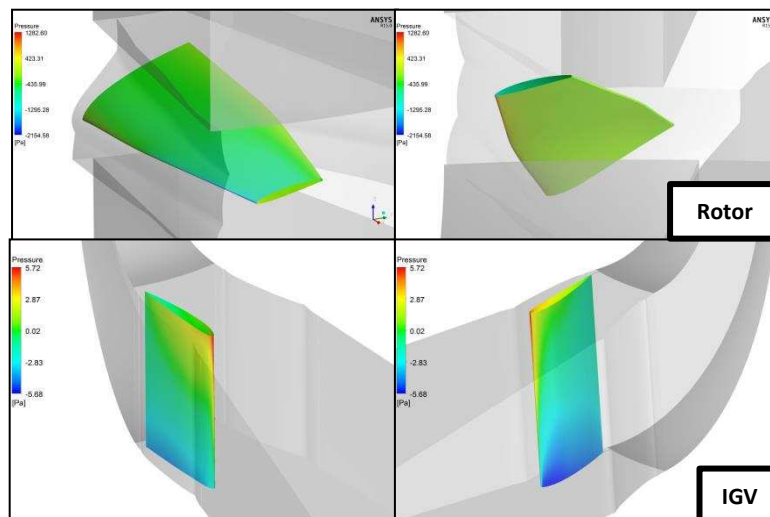


Figura 10: Pressure distribution on blades.

Tests performed were made in order to find a stable flow:

- Remesh: Meshed made in ANSYS Meshing and ANSYS ICEM CFD. NO SIGNIFICANT CHANGES.
- Interfaces: Frame Change: Stage > Frozen Rotor. NO SIGNIFICANT CHANGES

- Interfaces. Pitch Change: Automatic > Specified Pitch Angles. NO SIGNIFICANT CHANGES.
- Heat Transfer: Thermal Energy > Total Energy. NO SIGNIFICANT CHANGES.
- Timescale Control: Physical Timescale. RESULTS STRONGLY DEPENDENT ON TIMESCALE (see Chart 2).

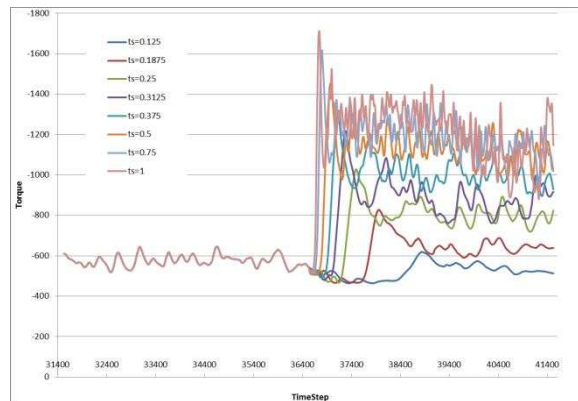


Chart 2: Temperature evolution in simulation in different timesteps.

Gannon turbine was designed for other operating conditions, very different from those present in Manzanares. This may be the reason why it was not possible to obtain a stable flow.

### 5. DEVELOPMENT OF FLURI'S TURBINE

Thomas Fluri has developed an exhaustive work with a horizontal axis turbine and IGV's both theoretical and experimentally. Four different multiple horizontal axis turbine configurations have been investigated. The turbine layouts studied are shown in the Figure 11 with a brief description of each layout presented is outlined below with aims to define the most feasible prior to simulation development:

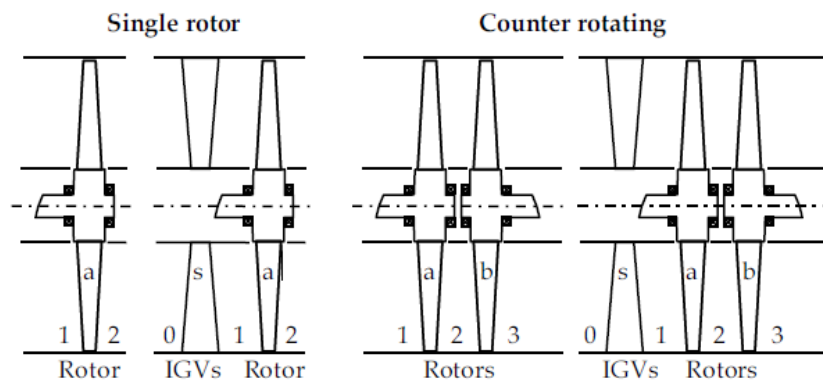


Figure 11: Schematic drawing of turbine layouts.

- Single rotor turbine without IGVs - The simplest layout. Its biggest disadvantage is that the swirl induced by the rotor cannot be recovered;
- Single rotor turbine with IGVs - The swirl is induced by guide vanes, which are located upstream of the rotor. The rotor operation turns the flow back to a close to axial direction;
- Counter rotating turbine without IGVs - The first rotor induces the swirl and the second rotor turns the flow back to a close to axial direction;
- Counter rotating turbine with IGVs - This is the most complex layout. The inlet guide vanes induce swirl in one direction. The first rotor turns the flow and induces swirl in the opposite direction. The second rotor finally turns the flow back to a close to axial direction.

A comparative analysis of different layouts has been performed by Fluri and Von Backström (Fluri & Von Backström, 2008b) and the efficiency prediction (see equations in Fluri T.P, 2008a) for various turbine layouts over a range of turbine speeds is shown in Chart 3. The main conclusion has been that counter rotating turbines performed better at speeds lower than 30 rpm with higher torque for the same shaft power. Thus, the single rotor turbine with IGV has the layout selected to represent Fluri's study in the simulation on Manzanares' scale by this work with regards to H-A's system.

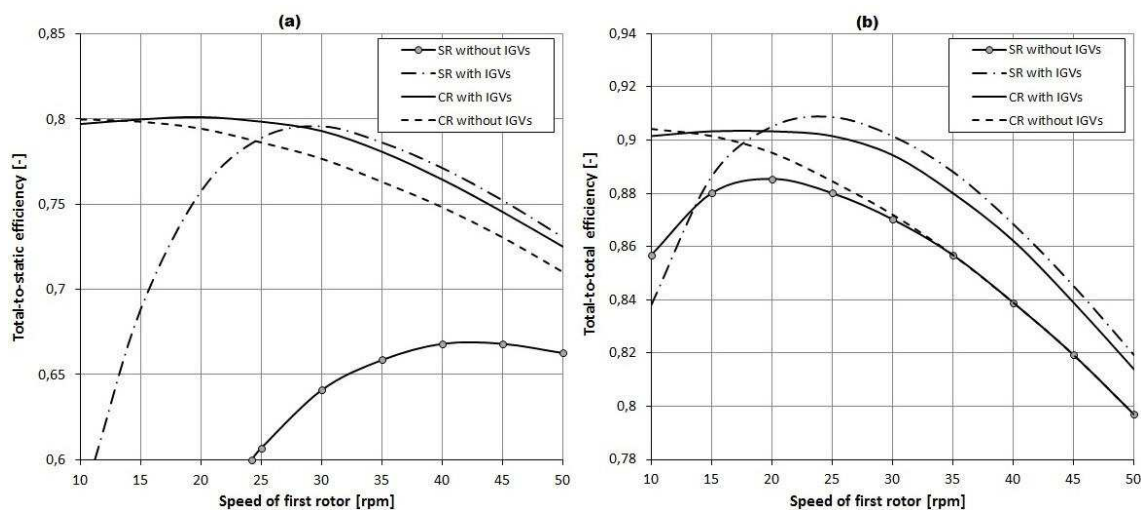


Chart 3: (a) Total-to-static and (b) total-to-total turbine efficiency prediction.

The main conclusion is that the single rotor layout without IGVs is the simplest and cheapest layout, however, its total-to-static efficiency is low because the swirl at the turbine exit cannot be recovered. All other layouts present much higher maximum total-to-static efficiency. Counter rotating turbines performed better at low speeds, which led to a higher torque for the same power output. Thus, the single rotor turbine with IGVs was the layout chosen by Fluri to study and it has been pointed as the design to be simulated in this work.

## 6. DESIGN OF FLURI'S TURBINE ON THE MANZANARES SCALE.

Table 1 presents all main parameters such as turbine diameter, the hub-to-tip ratio, the number of rotor blades and the tip speed for the multiple turbine rig were chosen to be the same as in the single turbine rig designed and built by Fluri.

Turbine diameter ( $D_t$ )	Hub-to-tip ratio ( $R_{HT}$ )	Number of rotor blades ( $Z_a$ )	Tip speed ( $U_a$ )
0.72 [m]	0.4	12	44.99 [m/s]

Table 1: Fluri's turbine design main parameters

The main assumptions for the turbine's design considered to the simulation model were zero exit swirl, free vortex design and constant axial velocity throughout the turbine. Based on these assumptions and laid on the Soderberg loss model flow angles were calculated. Flow angles are applied in the present modelling to identify the most adaptable geometry profile for the rotor blade and for the IGV.

It has been applied NACA 4-digit profiles and they were stacked on their gravity centers. The objective profiles are shown in the Figure 12 and defined parameters for the applied geometry have been summarized in the Table 2.

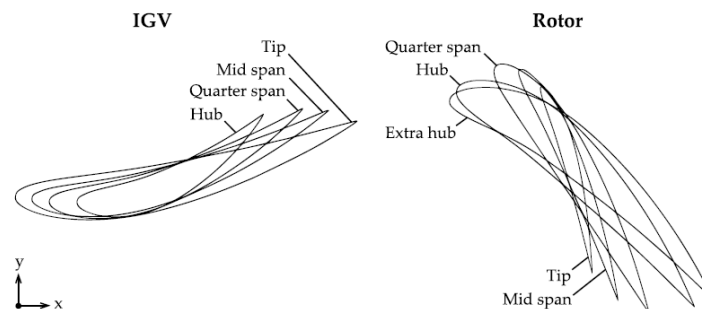


Figure 12: Sketch of IGV and rotor blade profiles.

		Position [mm]	Chord [mm]	Stagger [deg]	Blade profile
IGV	Hub	0.0	62.8	25.2	NACA 6416
	Quarter span	60.0	82.3	20.2	NACA 5414
	Half span	120.0	94.3	16.6	NACA 4412
	Tip	240.0	106.7	12.2	NACA 2411
Rotor	Extra hub	-13.9	97.5	-36.8	NACA 5416
	Hub	0.0	94.8	-42.7	NACA 4417
	Quarter span	54.0	85.0	-60.0	NACA 2415
	Half span	108.0	74.2	-70.5	NACA 1409
	Tip	216.0	56.8	-79.2	NACA 1408

Table 2: List of blade profiles parameters for Fluri's Turbine.

A 3D model of Fluri's design has been developed in this work considering all geometric details mentioned above. From this model, CFD simulations were performed aiming to compare results with experimental values measured on the physical prototype. The objective has been to guarantee the same performance prior to perform comparison with Manzanares scale.

Figure 13 shows the CAD geometry built by the commercial CFD software ANSYS Design Modeler and mesh generated by ANSYS Turbo Grid. The mesh for a single IGV and a single rotor blade had about a million of hexahedral elements.

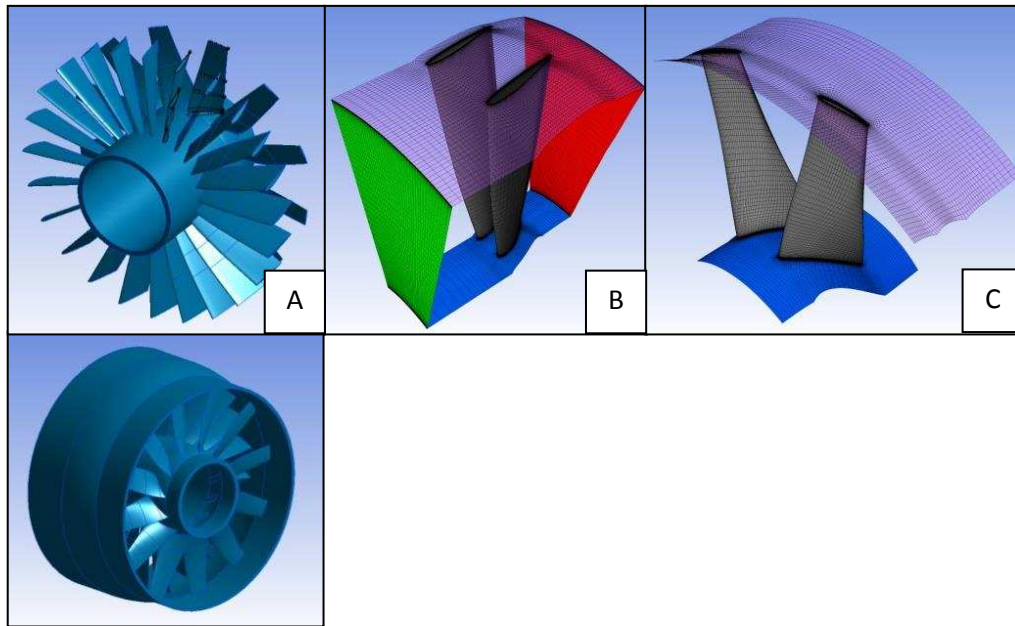


Figure 13: (a) IGV and Rotor geometry (b) IGV mesh (c) Rotor mesh.

The operating and boundary condition applied in the CFD simulations were the same as those applied in the experimental test. This information is provided in the Table 3.

Turbine speed [rad/s]	Volume flow rate [m <sup>3</sup> /s]	Inlet total temperature [K]	Inlet total pressure [Pa]
123.1	3.89	300	100,000

Table 3: Operating and boundary conditions.

CFD simulations and experimental measurements are shown in the graphs of the Chart 4. The graphs illustrate load coefficient, total-to-static efficiency and total-to-total efficiency for different values of flow coefficient (see equations in Fluri T.P, 2008a).

Two analyses have been performed with the commercial CFD software ANSYS CFX with a finer and a medium mesh, aiming to study the influence of the discretization. The results of both simulations presented low dispersion between themselves.

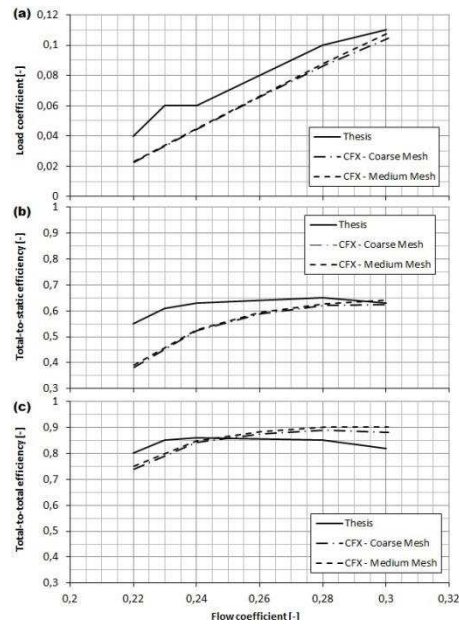


Chart 4: Values of (a) load coefficient, (b) total-to-static efficient and (c) total-to-total efficient versus flow coefficient for experimental and simulation results.

The differences between the CFD results and the experimental measurements were due to uncertainties on modeling taken into account how the profiles were assembled, the distance between IGV and rotor, the geometrical shape of the hub and shroud, the exact location where the rotor starts and the exact conditions (pressure, temperature, mass flow, etc.).

Dimensions of Fluri's turbine were modified to be coupled to the Manzanares scale. The system has been 5.55 times scaled up and a turbine diameter of 4 m was been modelled.

Figure 14 shows how the geometry has been designed providing details of Fluri's turbine to the Manzanares scale. A total of 12 axial turbines with horizontal axis have been placed around the chimney.

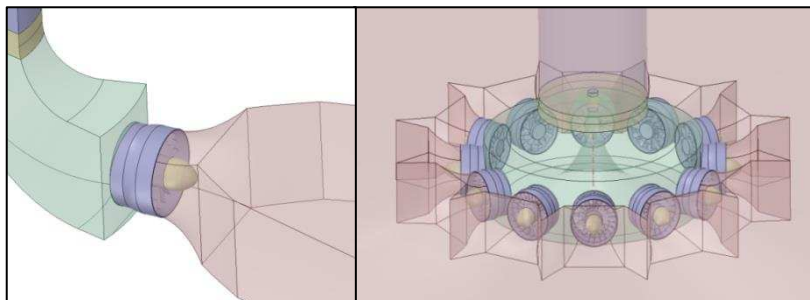


Figure 14: Geometry details of Fluri's system to Manzanares scale.

The mesh periodic volume of Fluri's turbine to the Manzanares is shown in the Figure 15. The developed mesh had about 25 millions of elements.

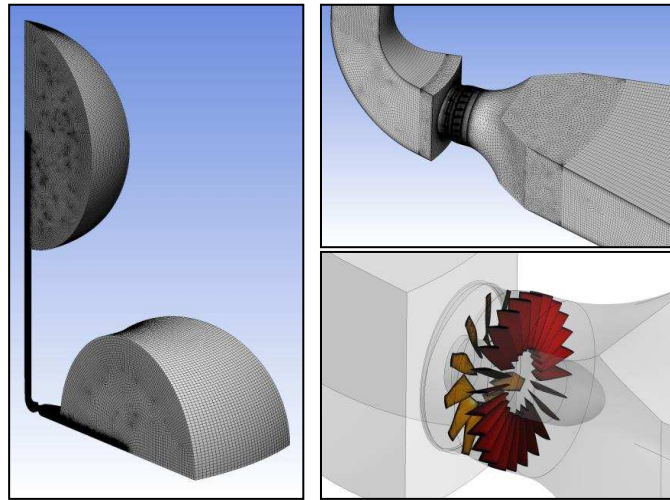


Figure 15: Mesh on periodic volume of Fluri's turbine to the Manzanares scale.

The best performances in case was torque: 300,9 [kN m] and 12 turbine power: 32,5 [kW].

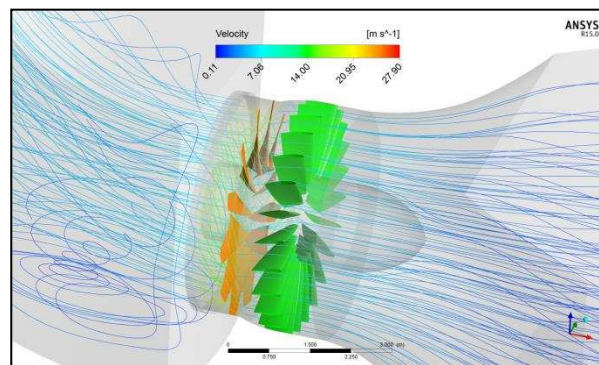


Figure 16: Streamlines through the rotor.

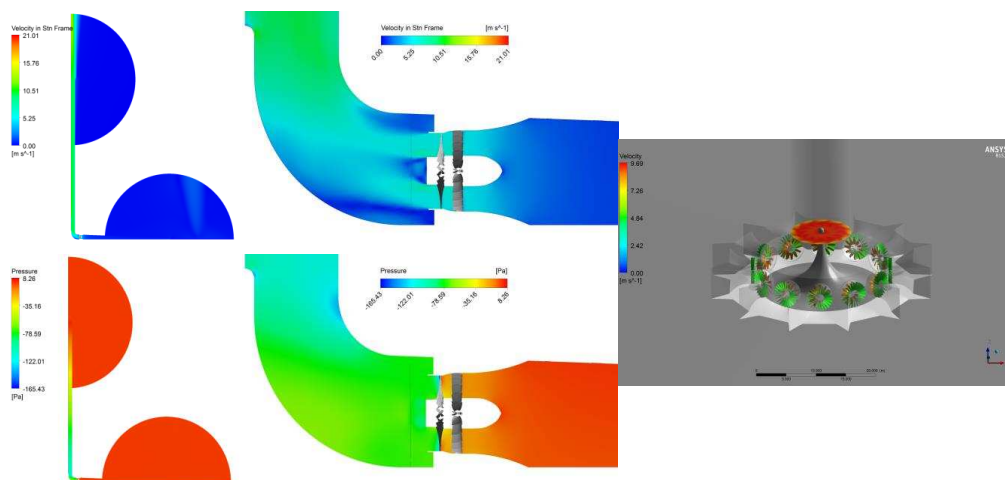


Figure 17: Velocity and pressure from simulation.

Maximum Power calculated available in chimney was

$$\text{Vel} = 9,26 \text{ [m/s]}$$

$$A = 80,28 \text{ [m}^2\text{]}$$

$$P_{av} = 39,4 \text{ [kW]}$$

It is possible to use a combination of a cluster arrangement of small turbines with a bigger axial turbine in the chimney. At the location of the plane shown in [Figure 16](#) and [Figure 17](#), the remaining power is about 40 kW.

## 7. FLURI OPTIMIZED DESIGN SIMULATION

Fluri designed his turbine for specific operating conditions, which differ significantly from the Manzanares plant. For this reason, an optimization process using the methodology *Adjoint Solver* of the commercial CFD software ANSYS Fluent 15.0 has been performed to the rotor. The *Adjoint Solver* lies on the sensitivity of a fluid system on a gradient-based shape optimization.

The *Adjoint Solver* methodology has been process aiming to maximize  $F_y$ , which directly affect the final torque, as it is illustrated in the [Figure 18](#).

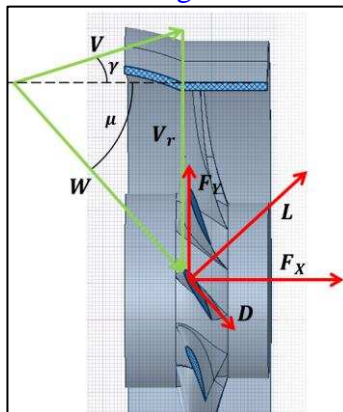


Figure 18: Forces applied to the rotor.

The optimization process with Adjoint solver has been performed by simulation of five 2D sections along the rotor blade span. [Figure 19](#) shows the comparison between the original sections and resulting sections of new design.

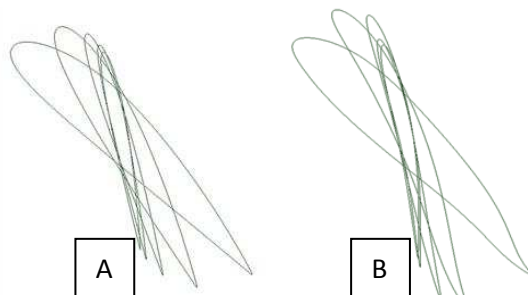


Figure 19: (a) Sections of Fluri's Design (b) Sections of Fluri's Optimized Design.

The results of torque and power for different rotational speeds are detailed in Table 4 (Fluri’s Design) and Table 5 (Fluri’s Optimized Design). The graph of Chart 5 show the torque of one turbine and the total power of 12 turbines for both rotors, original Fluri’s design and Fluri’s optimized design.

Case	$\omega$ [rad/s]	$\omega$ [rpm]	V [m/s]	Torque [N/m]	Power [W]	Power Turbine [kW]
1	4.45	42.5	4.89	294.00	1308.30	15.70
2	5.00	47.7	4.95	305.03	1525.13	18.30
3	7.50	71.6	4.96	317.48	2381.11	28.57
4	9.00	85.9	5.01	300.91	2708.19	32.50
5	10.00	95.5	5.06	262.27	2622.66	31.47
6	11.00	105.0	5.11	215.83	2374.14	28.49
7	15.00	143.2	5.33	-1.04	-15.60	-0.19

Table 4: Torque and power values for Fluri’s Design.

Case	$\omega$ [rad/s]	$\omega$ [rpm]	V [m/s]	Torque [N/m]	Power [W]	Power Turbine [kW]
1	7.75	74.0	4.24	261.18	2024.18	24.29
2	9.00	85.9	4.31	291.31	2621.80	31.46
3	10.00	95.5	4.22	299.20	2992.03	35.90

Table 5: Torque and power values for Fluri’s Optimized Design.

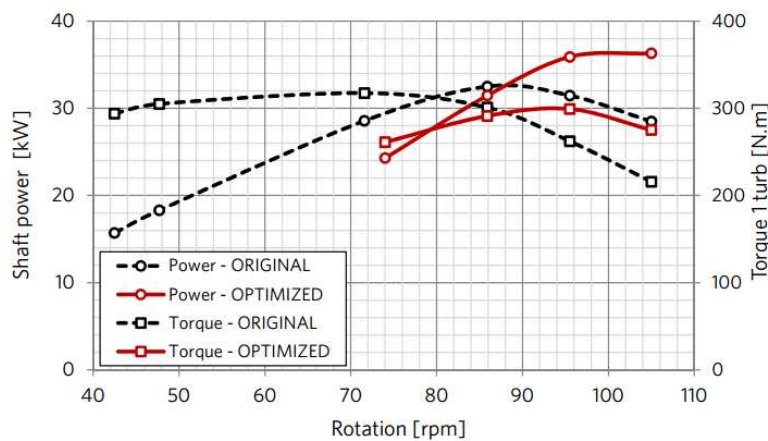


Chart 5: Axis torque (single turbine) and shaft power (12 turbines) of a single turbine versus angular velocity.

The shaft power of Fluri’s optimized design is about 12% higher than Fluri’s design for rotation higher than about 90 rpm. This is due to the longer edge of blades of the Fluri’s optimized design.

## 8. CONCLUSIONS

This work has shown a fair comparison between two different turbine application technologies to solar chimney power plant (SUPP): vertical-axis (single with IGV) and horizontal-axis (12 with IGV).

CFD simulation has allowed the redesign of both turbines' systems to the Manzanares scale and therefore compare to a real system. The upscaling methodology has faced necessary modifications to fit all devices within system positioning.

Results have shown that vertical-axis produce the energy peak of 78 kW at 58 rpm and that horizontal-axis produce the energy peak of 32,5 kW at 86 rpm. In comparison to the energy achieved from Manzanares' plant (35 kW), the vertical-axis simulated in this work has presented a much higher performance and indicates promising work.

Although the vertical-axis with 12 blades on the rotor and 18 blades on the IGV presented highest shaft power on the CFD simulation in comparison to the horizontal-axis system, both can be still combined to produce the maximum kinetic energy available.

**REFERENCES**

- ANSYS-Inc.. ANSYS Fluent Adjoint Solver. *Canonsburg, PA: Release 15.0*. November, 2013
- Denantes, F., & Bilgen, E.. Countering-rotating turbines for solar chimney power plants. *Renewable Energy 31*, 1873-1891, 2006
- Dhahri, A., & Omri, A.. A review of solar chimney power generation technology. *International Journal of Engineering and Advanced Technology (IJEAT)*, vol. 2, issue 3, 1-17, 2013
- Fluri, T. P.. Turbine layout and optimization solar chimney power conversion units. Stellenbosch: Department of Mechanical and Mechatronic Engineering. *University of Stellenbosch*, 2008a
- Fluri, T. P., & Von Backström, T. W.. Comparison of modelling approaches and layouts for solar chimney turbines. *Solar Energy 82*, 239-246, 2008b
- Fluri, T. P., & Von Backström, T. W.. Performance analysis of the power conservation unit of a solar chimney power plant. *Solar Energy 82*, 999-1008, 2008c
- Gannon, A. J.. Solar chimney turbine performance. Ph.D. Thesis. Stellenbosch: *Department of Mechanical Engineering. University of Stellenbosch*, 2002
- Gannon, A. J., & Von Backström, T. W.. Solar chimney turbine performance. *Journal of Solar Energy Engineering*, vol. 125, 101-106, 2003
- Ming, T. Z., Liu, W., Xu, G. L., Xiong, Y. B., Guan, X. H., & Pan, Y.. Numerical simulation of the solar chimney power plant systems coupled with turbine. *Renewable Energy 33*, 897-905, 2008
- Pretorius, J. P.. Solar tower plant performance characteristics. Stellenbosch: Department of Mechanical Engineering. *University of Stellenbosch*, 2004
- Pretorius, J. P., & Kröger, D. G.. Critical evaluation of solar chimney power plant performance. *Solar Energy 80*, 535-544, 2006
- Schlaich, J.. The solar chimney. *Stuttgart: Axel Manges*, 1995
- Von Backström, T. W., & Gannon, A. J.. Solar chimney turbine characteristics. *Solar Energy*, vol. 76, 235-241, 2004